THE JOURNAL OF PHYSICAL CHEMISTRY B

ARTICLE

pubs.acs.org/JPCB

# Effect of Galactosylceramide on the Dynamics of Cholesterol-Rich Lipid Membranes

Anette Hall,[†] Tomasz Róg,[†] and Ilpo Vattulainen[*,†,‡,§]

[†]Department of Physics, Tampere University of Technology, P.O. Box 692, FI-33101 Tampere, Finland

[‡]Department of Applied Physics, Aalto University School of Science, Espoo, Finland

[§]MEMPHYS—Center for Biomembrane Physics, University of Southern Denmark, Odense, Denmark

**ABSTRACT:** We use atom-scale molecular dynamics simulations to clarify the role of glycosphingolipids in the dynamics of cholesterol-rich lipid rafts. To this end, we consider lipid membranes that contain varying amounts of galactosylceramide (GalCer), sphingomyelin, cholesterol, and phosphatidylcholine. The results indicate that increasing the portion of GalCer molecules greatly slows down the lateral diffusion. Only 5−10 mol % of GalCer causes a decrease of almost an order of magnitude compared to corresponding membranes without GalCer. The slowing down is not related to interdigitation, which becomes weaker with increasing GalCer concentration. Instead, the decrease in diffusion is found to correlate with the increasing number of hydrogen bonds formed between GalCer and the phospholipid molecules, which is also observed to have other effects, such as to increase the friction between the membrane leaflets.

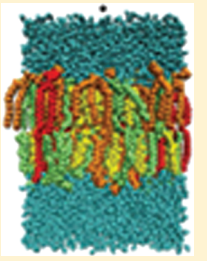

## INTRODUCTION

Glycolipids represent one of the most complex and the least understood lipid classes.[1] They are characterized by a glyco headgroup that is typically attached to glycerol or sphingosine, which in turn are connected to hydrocarbon chains via ester or ether bonds. The variety of different glycolipids is strikingly extensive. Even the broad distribution of hydrocarbon chain lengths and their levels of unsaturation suggest that the number of different glycolipids is substantial, yet this is just the tip of an iceberg. The main reason for the diversity of glycolipids lies in the headgroup region, since not only the number of different glyco headgroups is large but also their stereochemistry, connectivity, and the length of the chain formed of individual glyco units are exceptionally diverse.[2]

From a physical point of view, studies of glycolipids and their properties are challenging since the details of glycolipids truly make a difference. For example, it has been found that single-component lipid membranes composed of either galactose- or glucose-based glycerolipids have considerably different packing properties.[3,4] Yet the structures of galactose and glucose differ only in their stereochemistry at position 4 of the sugar ring. Given this, it is rather natural to appreciate that in cell membranes glycolipids are responsible for specific functions such as recognition and signaling.[2]

The present understanding of cell membranes' functions is largely based on the lipid raft model,[5−9] where a number of membrane functions are associated with membrane domains known as lipid rafts rich in cholesterol, saturated sphingolipids, and glycolipids. Some cell surface proteins bound with glycosyl phosphatidylinositol (GPI) anchors are also known to partition into lipid raft domains.[10] The concentration of glycolipids in the plasma membrane of all cells in higher animals ranges from 5 to 20 mol % and is enriched in lipid raft areas.[5,11] Based on experimental data, it has been found that glycosphingolipids (GSLs) interact favorably with cholesterol in the presence of sphingomyelin, but are unable to form sterol-enriched domains in its absence.[12,13] Recent studies have shown that cholesterol can modulate the receptor activity of GSLs through specific interactions.[14] Specific interactions between certain glycolipids and membrane proteins have also been suggested.[15] Altogether, the view which has emerged rather recently to appreciate the structural role of glycolipids in lipid membranes[16] is encouraging, but there remains the very limited understanding of the role of glycolipids in the dynamics of raftlike membrane domains.

Considering that the understanding of glycolipids' properties and their interactions with other abundant lipid species is very limited, there is increasing interest to elucidate these topics in great detail. Experimentally, this is difficult since there are not many techniques able to characterize molecular phenomena with sufficient time and spatial resolution. Meanwhile, atomistic simulations are the method of choice for this purpose since the present models with current computing resources provide a means to explore very specific processes in full atomic detail, over reasonably long time scales of the order of microseconds or even milliseconds.[17,18] What is more, atomistic simulations can shed light not only on structure, but especially on nanoscale dynamics taking place in many-component membranes with and without membrane proteins.[19,20]

In this work, we use atomistic simulations to unravel the role of glycosphingolipids in dynamical properties of cholesterol-rich raftlike membranes consisting of cholesterol (CHOL), palmitoylsphingomyelin (SM), palmitoyloleoylphosphatidylcholine (POPC), and galactosylceramide (GalCer). We find a number of intriguing observations. To start with, lateral diffusion is observed to

**Received:** April 7, 2011
**Revised:** October 25, 2011
**Published:** October 27, 2011

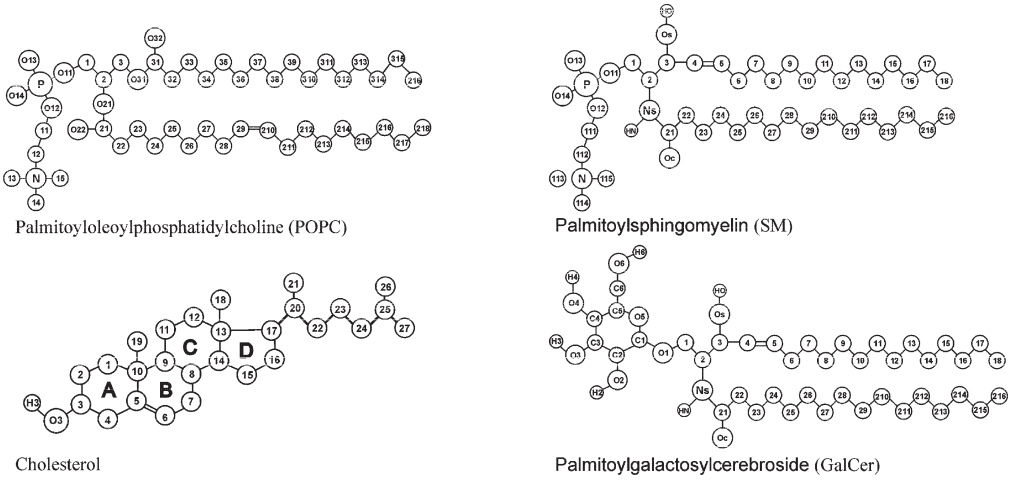


**Figure 1.** Schematics of the simulated molecules.

substantially slow down in the presence of GalCer, the lateral diffusion of GalCer being the slowest and the diffusion of cholesterol being the fastest of all the lipids in a membrane. Correspondingly, the friction between the two monolayers in a lipid bilayer is found to increase for increasing GalCer concentration, which is not surprising. However, the cause of the increase in friction and slowing down of diffusion is unclear. One is tempted to assume that they would be due to an increase in interdigitation, but instead we find interdigitation to slightly decrease for increasing galactosylceramide concentration. The cause of the changes in the dynamics turns out to lie mainly in the strong hydrogen-bonding capacity of GalCers that leads to the many observed consequences for the dynamics.

## METHODS

**Simulation Details.** This work compares six lipid bilayer systems containing galactosylceramide, sphingomyelin, cholesterol, and palmitoyloleoylphosphatidylcholine. These molecules are shown in Figure 1. The first three of these systems having approximately 5 mol % of GalCer have been presented in a previous work.[21] The three new systems have similar compositions of SM, CHOL, and POPC, but with double the amount of GalCer (approximately 10 mol %). Exact system compositions for each of these systems are shown in Table 1. All the systems have a total number of 256 lipids. Systems $I_{10}$ and $I_5$ have POPC, SM, and CHOL in approximately equal amounts. Systems $II_{10}$ and $II_5$ have double the amount of POPC, and systems $III_{10}$ and $III_5$ do not contain SM or CHOL at all. In this article, we refer to I when the concentration of GalCer is not specified (representing $I_5$ and $I_{10}$), and II and III are considered similarly.

For all molecules, we applied the same united atom model as used in our previous article.[21] The force field parameters of the model for POPC,[22] SM,[23] CHOL,[24] and GalCer[21] were all obtained from earlier studies, with the unsaturated part of POPC modified to better account for the conformational degrees of freedom[25−27] associated with the double bond region. The model used for water was SPC.[28] The starting configurations for the new systems were randomly generated using PACKMOL,[29] using the same molecular configurations as in the previous work.[21] After the addition of water to the systems, their energy was minimized with the steepest descent algorithm.

All of the simulations were performed with classical atomistic molecular dynamics using the GROMACS software package

**Table 1. System Compositions for the Studied Six Systems[a]**

| system | GalCer | CHOL | SM | POPC | water | phase |
|---|---|---|---|---|---|---|
| $I_{10}$ with 10 mol % GalCer | 24 | 78 | 76 | 78 | 9789 | $l_o$ |
| $II_{10}$ with 10 mol % GalCer | 24 | 58 | 58 | 116 | 9413 | $l_o$ |
| $III_{10}$ with 10 mol % GalCer | 24 | 0 | 0 | 232 | 10287 | $l_d$ |
| $I_5$ with 5 mol % GalCer | 12 | 82 | 80 | 82 | 6110 | $l_o$ |
| $II_5$ with 5 mol % GalCer | 12 | 62 | 62 | 120 | 7944 | $l_o$ |
| $III_5$ with 5 mol % GalCer | 12 | 0 | 0 | 244 | 8655 | $l_d$ |

[a] The systems containing 5 mol % GalCer have been presented in a previous work.[21] $l_o$ stands for the liquid-ordered phase, and $l_d$ for liquid disordered.

versions 3.3 (for the first 100 ns) and 4.0.3, available under the GNU General Public License from www.gromacs.org.[30−32] All of the used simulation parameters for a GalCer concentration of 10 mol % were the same as what were used in the earlier simulations with 5 mol % of GalCer.[21] The simulations were conducted in the NpT ensemble, with the temperature at 310 K and semi-isotropic pressure at 1 bar. The systems were equilibrated for a period of 20 ns using the Berendsen thermostat and barostat[33] with a time constant of 0.1 ps, after which the Nosé−Hoover[34,35] thermostat and Parrinello−Rahman[36,37] barostat with a time constant of 1 ps were used for the rest of the simulations. Total simulation time for each simulation was 200 ns, with a time step of 2 fs. All of the bonds in the systems were constrained using the LINCS algorithm.[38] The van der Waals interactions were calculated to a cutoff radius of 1 nm, and for Coulomb interactions the reaction field (RF) method[39] was employed with a truncation distance of 2 nm and a dielectric constant of 80. The RF technique was chosen for electrostatics to be on equal footing with earlier simulations,[21,40] which in turn showed that its results are consistent with other schemes for electrostatics such as PME.[21]

**Analysis.** Since the systems were found to take approximately 100 ns to equilibrate, only the last 100 ns of the simulations were used for analysis.

Average area per lipid has been calculated by dividing the total area of a membrane by the number of lipids in a monolayer. Bilayer thickness was calculated from the peak-to-peak distance of the electron density distribution of all the atoms in the system.

To characterize the dynamics of lipids in the bilayer, we calculated the lateral diffusion coefficient $D$:

$$D = \lim_{t \to \infty} \frac{\langle [\vec{r}(t + t_0) - \vec{r}(t_0)]^2 \rangle}{4t} \quad (1)$$

Here, the coordinates $\vec{r}$ are the centers of mass of the lipid molecules, for which the time evolution is examined. In the analysis, the motion of lipids is here considered with respect to the motion of the monolayer's center of mass. This is a commonly used means to avoid artifacts due to monolayer motion, since in simulations of membranes the two monolayers may move with respect to each other, and this artifact has been observed to be particularly severe if long-range electrostatic interactions are treated incompletely.[41,42] However, since it is not self-evident that this strategy is always valid in simulations over a rather short time scale, care in interpreting the results is often justified. In the present study, we confirmed that the lipid diffusion coefficients were essentially identical when they were computed with the above scheme, taking the monolayer's center of mass motion into account, and when they were determined without consideration of this feature.

Intermonolayer friction (viscosity) for a similar system has been previously characterized by computing the relative motion of the two monolayers in the system, and calculating their diffusion with respect to each other.[43] In this work, we have followed a similar approach to obtain a measure for the shear viscosity of the membrane leaflets with respect to one another by plotting the average relative mean-squared displacement between the two monolayers as a function of time, and calculating the respective diffusion coefficient. Here, one should mention that this measure gauges the friction between the two monolayers rather than the true viscosity within a membrane, thus in the discussion below we refer to "friction" when we discuss this aspect of our work.

Interdigitation of the lipid tail ends between the two monolayers was studied through the integral[44]

$$\lambda_{ov} = \int_0^L \rho_{ov}(z)\, dz \quad (2)$$

of the overlap parameter $\rho_{ov}(z)$ over the simulation box. The overlap parameter as a function of $z$-coordinate (along the membrane normal direction) is defined as[44]

$$\rho_{ov}(z) = 4\frac{\rho_t(z)\rho_b(z)}{[\rho_t(z) + \rho_b(z)]^2} \quad (3)$$

where $\rho_t(z)$ and $\rho_b(z)$ refer to the number densities of atoms belonging to the top and bottom layers, respectively. The overlap parameter $\rho_{ov}$ has a value of zero when there is no overlap between the two layers, and a value of 1 if half of the density is from the top and half from the bottom layer.

$\lambda_{ov}$ is a single length scale that can be used to compare the amount of interdigitation between different systems.[44] In an ideal case where in all interdigitating areas there is an equal number of atoms from both leaflets, it would be identical to the length (along the membrane normal direction) of the region where interdigitation takes place.

The deuterium order parameters were calculated with the second-order Legendre polynomial

$$S_{CD} = \frac{1}{2}\langle 3\cos^2\theta - 1 \rangle \quad (4)$$

**Table 2. Area per Lipid and Bilayer Thickness of the Systems Compared to Those from a Previous Study[21]**

| system | area per lipid (nm$^2$) | bilayer thickness (nm) |
|---|---|---|
| $I_{10}$ | 0.406 ± 0.003 | 4.66 ± 0.02 |
| $II_{10}$ | 0.434 ± 0.004 | 4.66 ± 0.02 |
| $III_{10}$ | 0.641 ± 0.008 | 3.60 ± 0.02 |
| $I_5$ | 0.408 ± 0.003 | 4.56 ± 0.02 |
| $II_5$ | 0.445 ± 0.004 | 4.42 ± 0.02 |
| $III_5$ | 0.660 ± 0.008 | 3.60 ± 0.02 |

from the angles $\theta$ between a selected C−H vector and the bilayer normal. Since hydrogens are not explicitly included in the present united atom model, their positions were reconstructed to the molecules before analysis, assuming ideal positions in the given geometries.

Rotational motions of the headgroup, the interfacial region, and the acyl chain part of a membrane were measured through the reorientational autocorrelation function:

$$C(t) = \frac{1}{2}\langle 3[\vec{\mu}(t)\cdot\vec{\mu}(0)]^2 - 1 \rangle \quad (5)$$

where $\vec{\mu}(t)$ is a unit vector that defines the rotational mode in question. In practice, the headgroup vector is defined as the vector from the phosphorus to the nitrogen atom for the phospholipids, and from the carbon atom connecting the sugar ring with the rest of the molecule to the one opposite it in the ring for the glycolipid. The interface vector is defined as the vector from the sn-1 glycerol carbon to the sn-3 glycerol carbon for POPC, and similarly the corresponding carbons in the sphingosine part of the ceramides for the two sphingolipids. Finally, for the acyl chain the vector is defined as the vector from the first carbon after the carbonyl carbon to the chain end in phospholipids, and for the sphingosine chains it is from the double-bonded carbon next to the one bonded to the OH group, and then to the end of the chain.

Existence of hydrogen bonds between lipid components is judged on geometrical criteria,[45] where (a) the distance between a donor and an acceptor is less than or equal to 0.325 nm and (b) the angle between the vector linking the donor group with the acceptor group and the vector formed by the chemical donor-hydrogen bond is smaller than 35°. Presence of charge pairs[46] between negatively charged oxygen atoms and positively charged choline methyl groups is based on a cutoff distance of 0.4 nm.

## RESULTS

**Membrane Dimensions.** The calculated area per lipid and bilayer thickness for the 10% GalCer systems simulated here, together with those obtained from the previous study on 5% systems,[21] are presented in Table 2. Overall the area per lipid slightly decreases as the number of GalCer molecules is doubled. This is clearly seen in the liquid-disordered systems (III), while the most ordered systems (I) exhibit very little change in the area per lipid. The bilayer thickness on the other hand increases with more GalCer for the liquid-ordered systems I and II. The change is greater for II, leading to the two 10% liquid-ordered systems ($I_{10}$, $II_{10}$) having the same bilayer thickness.

**Lateral Diffusion.** Table 3 presents the overall diffusion coefficients of the 5%[21] and 10% GalCer systems. As the amount of GalCer is doubled, diffusion in the systems slows down considerably. The change is most drastic for the 10% system $I_{10}$ where

the diffusion coefficient drops to one-fifth of the corresponding value in the 5% system. For the system $II_{10}$ the diffusion coefficient decreases by over two-thirds, and for $III_{10}$ by nearly a half.

For comparison, for the same model but without GalCer, the lateral diffusion coefficient has been observed to be[40] $0.037 \pm 0.002$ cm$^2$/s in the system I, $0.08 \pm 0.02$ cm$^2$/s in II, and $0.67 \pm 0.06$ cm$^2$/s in III.

**Table 3. Lateral Diffusion Coefficients of the Lipids As Averaged over All Lipids in the Systems**[a]

| system | diffusion ($10^{-7}$ cm$^2$/s) |
|---|---|
| $I_{10}$ | $0.009 \pm 0.004$ |
| $II_{10}$ | $0.018 \pm 0.006$ |
| $III_{10}$ | $0.34 \pm 0.04$ |
| $I_5$ | $0.047 \pm 0.003$ |
| $II_5$ | $0.065 \pm 0.005$ |
| $III_5$ | $0.55 \pm 0.03$ |

[a] The results for the present study are compared to those from a previous study.[21]

**Table 4. Lateral Diffusion Coefficients for Each Lipid Component in the Simulated Systems Compared to Ones from a Previous Study**[21] [a]

| system | $D_{GalCer}$ | $D_{CHOL}$ | $D_{POPC}$ | $D_{SM}$ |
|---|---|---|---|---|
| $I_{10}$ | $0.009 \pm 0.003$ | $0.010 \pm 0.002$ | $0.010 \pm 0.003$ | $0.009 \pm 0.004$ |
| $II_{10}$ | $0.009 \pm 0.007$ | $0.026 \pm 0.007$ | $0.017 \pm 0.005$ | $0.017 \pm 0.007$ |
| $III_{10}$ | $0.18 \pm 0.04$ | | $0.36 \pm 0.04$ | |
| $I_5$ | $0.025 \pm 0.004$ | $0.053 \pm 0.004$ | $0.056 \pm 0.004$ | $0.035 \pm 0.004$ |
| $II_5$ | $0.046 \pm 0.008$ | $0.07 \pm 0.02$ | $0.070 \pm 0.005$ | $0.057 \pm 0.004$ |
| $III_5$ | $0.34 \pm 0.08$ | | $0.56 \pm 0.03$ | |

[a] The results are given in units of $10^{-7}$ cm$^2$/s.

**Table 5. Lateral Diffusion Coefficients from the Mean-Squared Displacement of the Relative Motion of the Two Monolayers, on a 50 ns Time Scale Analyzed for the Last 100 ns of the Simulation**

| system | diffusion ($10^{-7}$ cm$^2$/s) |
|---|---|
| $I_{10}$ | $0.0 \pm 0.4$ |
| $II_{10}$ | $0.7 \pm 0.6$ |
| $III_{10}$ | $0.7 \pm 0.7$ |
| $I_5$ | $0.5 \pm 0.3$ |
| $II_5$ | $0.6 \pm 0.5$ |
| $III_5$ | $1.7 \pm 1.1$ |

A breakdown of the average diffusion coefficients of individual lipid components in each of the systems is shown in Table 4. In all of the systems with 10% GalCer, each lipid component has a smaller diffusion coefficient than in the corresponding system with 5% GalCer. GalCer is the lipid component with the clearly smallest diffusion coeffient in all systems, except system $I_{10}$, where all components have approximately the same diffusion coefficient. In both of the 10% liquid-ordered systems ($I_{10}$ and $II_{10}$) the diffusion coefficient of GalCer has the same value. In system $II_{10}$ the SM and POPC molecules diffuse two times and the CHOL molecules three times as fast as GalCer. For the system $III_{10}$ with 10% GalCer, the diffusion coefficient of POPC is twice as large as that of GalCer.

**Interleaflet Friction.** Friction between the two monolayers was studied through the relative mean-squared displacement of the two monolayers, as a function of time. Diffusion coefficients calculated from the average slope of the displacement curves are shown in Table 5, along with error bounds estimated from changes in the slope of the mean-squared displacement.

The diffusion coefficient for the system $I_{10}$ with 10% GalCer calculated on this time scale has a value of zero, as the two monolayers in the system are unable to diffuse freely relative to each other. This can be observed from Figure 2A, which shows the average mean-squared displacement of the two layers as a function of time. In effect, the two monolayers of the bilayer are stuck to each other, with little room for movement if a short initial period of time is disregarded. On this shorter time scale up to 5 ns, the layers are able to diffuse more freely, reaching a mean-squared displacement of approximately 0.25 nm$^2$. During this short time period they reach an average diffusion coefficient of $1.1 \times 10^{-7}$ cm$^2$/s. However, the average movement of individual lipids is not restricted in this way as can be seen from Figure 2B. The diffusion of the lipid molecules is much slower, but stable.

According to Table 5, the system $III_5$ with 5% GalCer has clearly the largest diffusion coefficient for the relative movement of the monolayers. The other systems (excluding $I_{10}$) exhibit mostly similar values.

**Interdigitation.** Interdigitation for the systems was calculated through the number densities of the two monolayers using the method described in Analysis.[44] The obtained values for $\lambda_{ov}$ characterizing the range of interdigitation in each system are presented in Table 6.

The liquid-disordered systems III have notably more interdigitation than the liquid-ordered systems I and II. When the amount of GalCer in each system is increased from 5% to 10%,

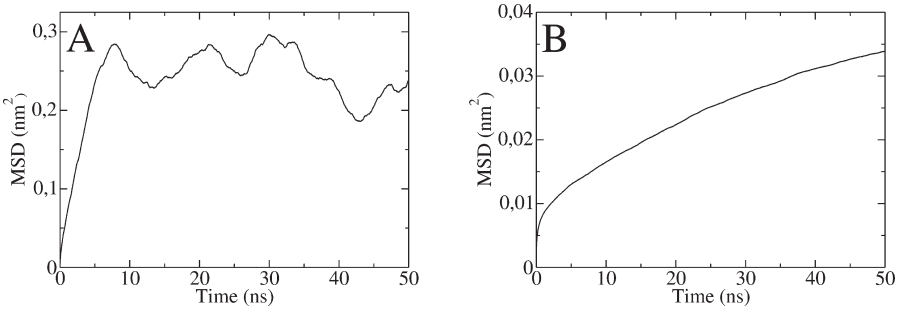


**Figure 2.** Panel A shows the mean-squared displacement (MSD) of the relative motion of the two monolayers in $I_{10}$, while panel B shows the averaged mean-squared displacement of the movement of all the individual lipid molecules in the same system.

the liquid-ordered systems exhibit slight decreases in interdigitation, most clearly seen in the membrane center region of the electron density profiles in II (Figure 3). For the liquid-disordered systems III, the amount of interdigitation is not affected by the change in GalCer. The greatest contribution to interdigitation comes from the GalCer molecules, which tend to reside deeper in the bilayer. This can be observed from the electron density distributions of the lipid components, as is shown in Figure 3 for the systems II.

**Table 6. Length Scale $\lambda_{ov}$ Characterizing the Range of Interdigitation Across the Monolayer−Monolayer Interface, As Calculated According to the Method Presented by Das et al.**[44]

| system | $\lambda_{ov}$ (nm) |
|---|---|
| $I_{10}$ | 0.22 ± 0.01 |
| $II_{10}$ | 0.25 ± 0.01 |
| $III_{10}$ | 0.53 ± 0.02 |
| $I_5$ | 0.24 ± 0.01 |
| $II_5$ | 0.31 ± 0.01 |
| $III_5$ | 0.53 ± 0.02 |

**Order Parameters.** Order parameters for the two carbon chains of the lipid molecules are depicted in Figure 4 for GalCer, Figure 5 for SM, and Figure 6 for POPC. Generally, the 10% systems are slightly more ordered than the 5% ones. The difference is the greatest in the systems II, especially for the GalCer sphingosine chain and the POPC sn-2 chain. In the systems III there is very little change in the ordering of the chains. Overall, the differences are quite small, indicating that the addition of GalCer from 5% to 10% does not greatly affect the ordering of the hydrocarbon chains.

**Rotational Autocorrelation Functions.** Autocorrelation functions (ACFs) of the rotational motion of the molecule provide information on the speed at which molecules orientation is rearranged. For the headgroups of the lipids considered here, the computed rotational ACFs are presented in Figure 7.

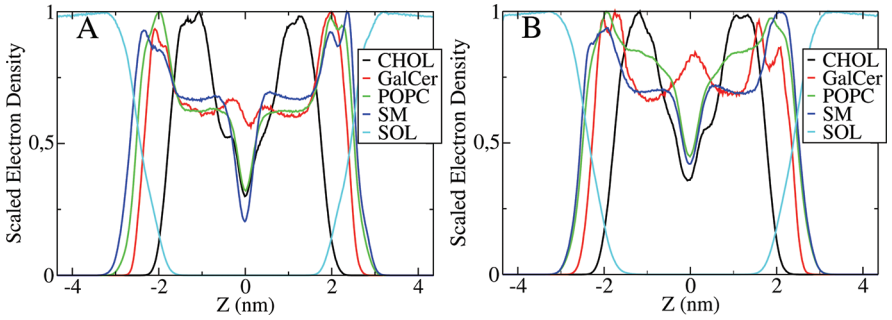


**Figure 3.** Comparison between the electron density distributions of systems $II_{10}$ (A) and $II_5$ (B).

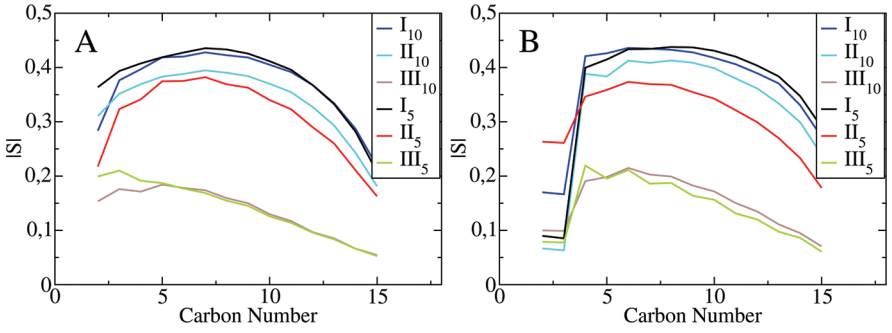


**Figure 4.** Order parameters ($S_{CD}$) for the GalCer acyl (A) and sphingosine (B) chains in each of the different systems. Small carbon numbers correspond to those close to the headgroup.

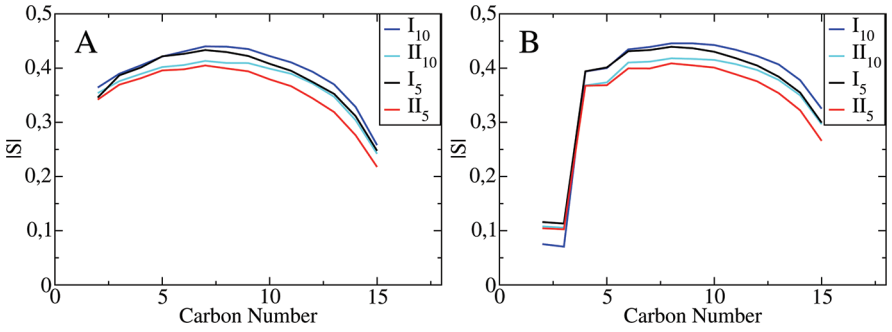


**Figure 5.** Order parameters ($S_{CD}$) for the SM acyl (A) and sphingosine (B) chains in systems I and II. Small carbon numbers correspond to those close to the headgroup.

The autocorrelation functions of the headgroup clearly tend to approach nonzero values at infinity, due to the headgroups not being able to move freely in all directions. Instead, the movement of the headgroups is restricted by their angle from the bilayer normal, with larger plateau values at asymptotically long times indicating less tilt.[44] For both headgroups, the ACFs of the 10% systems tend to approach larger limiting values than the corresponding systems with 5% GalCer, and thus the headgroup in these systems tends to be more closely aligned with the bilayer normal. Additionally, the phosphate headgroup in SM and POPC tends to exhibit clearly more tilt than the galactose headgroup in GalCer. Comparison between the ACFs for the vector along the galactose headgroup and the normal of its plane indicates that the normal of the headgroup can rotate more freely than the tip of the headgroup, and thus approaches a lower value at infinity. However, it should be noted that the headgroup rotational movement does not completely relax during the scope of these simulations, and thus cannot be quantitatively measured.

The most important result that can be seen from these results is that there is very little difference between the slopes of the 5% and 10% GalCer systems as a function of time, even though they are approaching different values. This piece of information is relevant, since the relaxation time $\tau_R$ characterizing rotational diffusion is usually determined from the long-time behavior that is assumed to decay in an exponential manner via $\mathrm{ACF}(t) \sim \exp(-t/\tau_R)$. Determination of $\tau_R$ is not appropriate here since the asymptotic values of $C(t)$ are not available. Yet the data for $C(t)$ indicate that the long-time relaxation of the rotational movement is not greatly affected by the increase in GalCer, unlike the diffusion of the individual system components. Essentially, the diffusion of the molecule as a whole and the long-time rotational motion of its headgroup are uncoupled.

Similar trends can be seen for the rotational ACFs of the interfacial regions of the molecules, shown in Figure 8. Again, the ACFs for systems with 10% GalCer seem to approach higher asymptotic values than those with 5% GalCer, but there is little difference in their relaxation times.

The ACFs for the rotational movement of the two different hydrocarbon chains in each molecule are shown in Figure 9. Unlike the headgroup and the interface, the chains reach their plateau value in the time scale of these simulations and thus have a significantly shorter relaxation time. This is quite well in line with

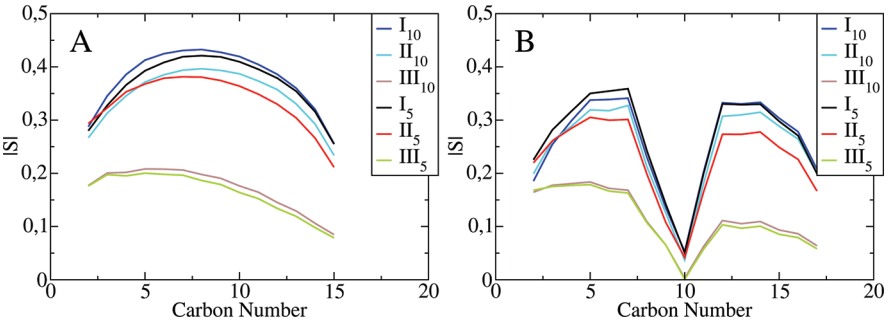


**Figure 6.** Order parameters ($S_{CD}$) for the POPC sn-1 (A) and sn-2 (B) chains in each of the different systems. Small carbon numbers correspond to those close to the headgroup.

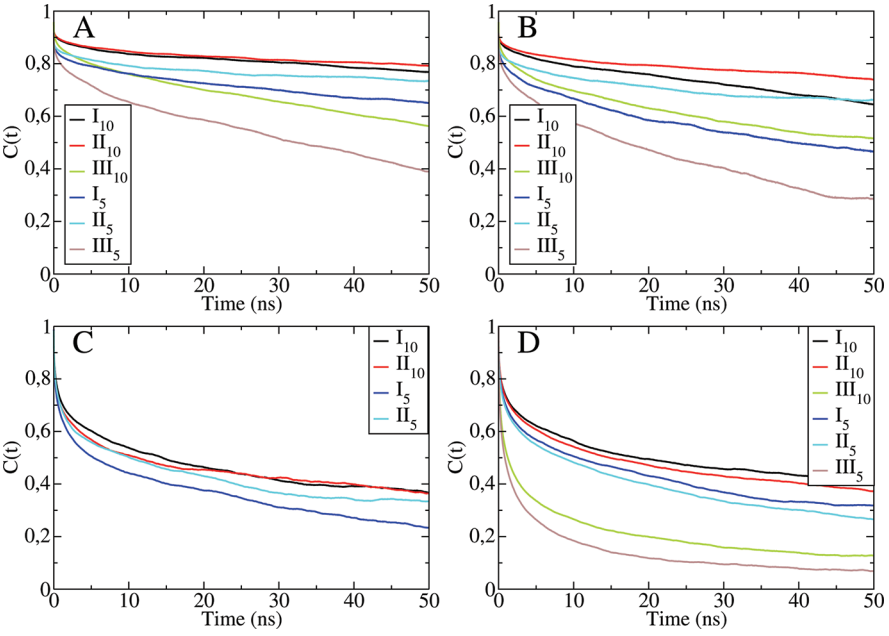


**Figure 7.** Headgroup rotational autocorrelation functions for GalCer (A), the normal of the plane for the GalCer sugar moiety (B), SM (C), and POPC (D).

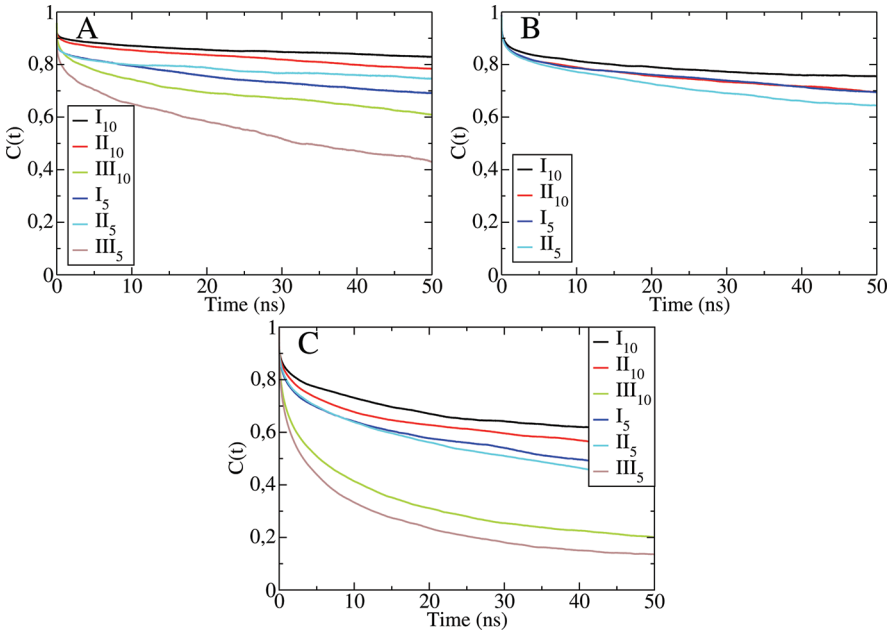


**Figure 8.** Interface rotational autocorrelation functions for GalCer (A), SM (B), and POPC (C).

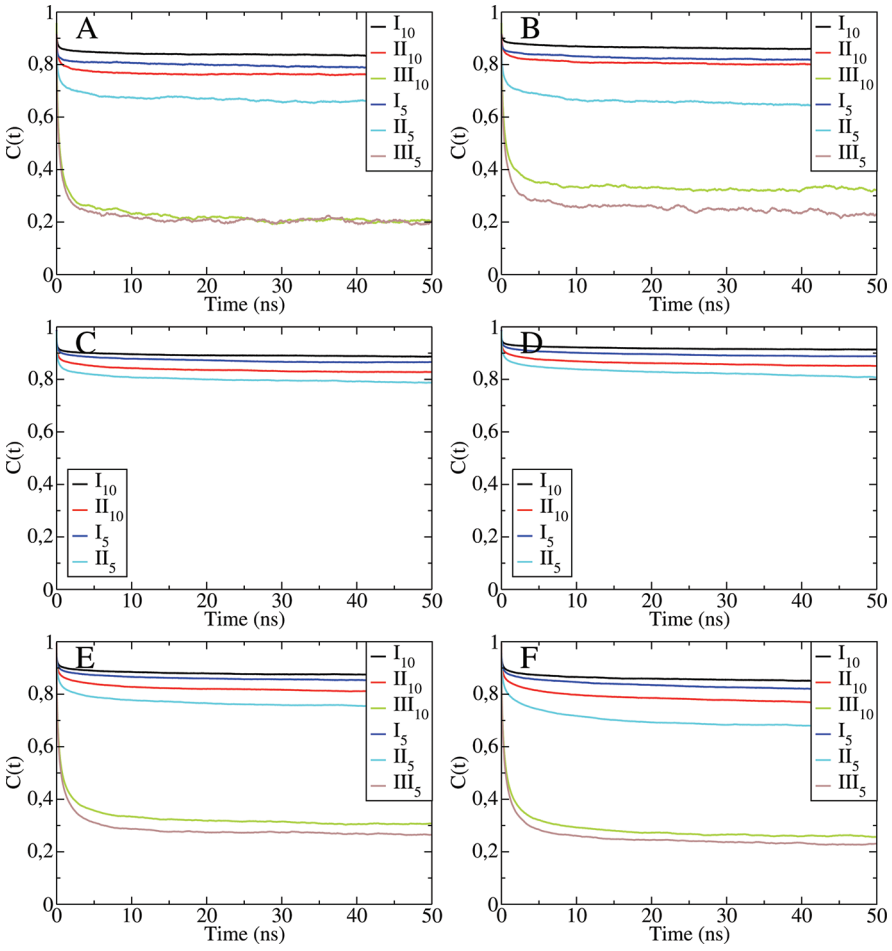


**Figure 9.** Chain rotational autocorrelation functions for the GalCer acyl (A), GalCer sphingosine (B), SM acyl (C), SM sphingosine (D), POPC *sn*−1 (E), and POPC *sn*−2 (F) chains.

previous results for lipids.[47] These results show even more clearly that there is no major change in relaxation times caused by the addition of GalCer to the systems. Similarly to the headgroups and interfacial regions, the chains in the 10% GalCer systems are more aligned with the bilayer normal than in the similar 5% systems, in agreement with the $S_{CD}$ data in Figures 4−6.

**Hydrogen Bonding and Charge Pairs.** Table 7 shows the average number of hydrogen bonds around the different lipid molecules. The data for the 5% systems is from the previous article.[21]

As can be seen from the results, GalCer molecules have the largest number of hydrogen bonds to other molecules, due to their sugar headgroups. The increase in GalCer from 5% to 10% in I seems to lead to a clear decrease in GalCer−SM bonds and increase in GalCer−POPC bonds. However, there is only a slight decrease in the total number of hydrogen bonds from GalCer to POPC and SM—the number of hydrogen bonds to phospholipids seems to be maintained. In the systems II the increase in GalCer leads to more bonds with SM molecules, and a slight increase in overall bonds with either POPC or SM. Additionally, the number of bonds from GalCer to CHOL is decreased somewhat.

The addition of more GalCer seems to have very little effect on the hydrogen bonding of CHOL molecules in I, but in the systems II there is an increase in the number of bonds to POPC molecules associated with the increase in GalCer. This is not instantly visible from Table 7, but rather from the number of bonds between an average CHOL−POPC pair in the same leaflet, which changes from 0.012 to 0.014. Additionally bonds from SM to POPC are slightly increased in both I and II.

The total number of hydrogen bonds from POPC molecules greatly increases in all of the systems with the change from 5% to 10% GalCer. There is also a small increase in the number of hydrogen bonds for both SM and CHOL molecules in the systems II.

Calculated charge pairs for all of the simulated systems are presented in Table 8. The results show that GalCer tends to favor formation of charge pairs with POPC over SM in both of the liquid-ordered systems (I, II) regardless of the number of GalCer molecules, even when taking the differing numbers of SM and POPC into account. In the systems I, the number of CHOL−SM and CHOL−POPC charge pairs is somewhat equal, while in the 10% system $II_{10}$ the number of CHOL−POPC pairs is a bit larger, even when taking the possible number of molecule pairs into account. Most importantly, the number of CHOL−POPC bonds in the 5% system $II_5$ is much smaller than would be expected from the other results. Generally, SM forms a higher total number of charge pairs than POPC. Interestingly however, SM molecules have their lowest number of charge pairs in the most ordered system ($I_{10}$) and highest number in the 4-component system with the least ordering ($II_5$). If we take the relative number of lipids into account, the most common charge pairs are from SM to SM, but this may be affected by the tendency of SM molecules to form intramolecular charge pairs. The most notable difference between systems containing 5% and 10% of GalCer is a decrease in charge pairs formed between SM and POPC molecules, when the number of GalCer molecules is increased. This is most clearly visible for the systems I where the small decrease in the number of SM and POPC molecules is not able to explain the large decrease in POPC−SM charge pairs.

**Table 7. Average Number of Hydrogen Bonds from a Molecule of One Species to Molecules of the Second Type[a]**

| | system | | | | | |
|---|---|---|---|---|---|---|
| molecule pair | $I_{10}$ | $II_{10}$ | $III_{10}$ | $I_5$ | $II_5$ | $III_5$ |
| GalCer−GalCer | 0.33 | 0.34 | 0.23 | | | |
| GalCer−POPC | 2.55 | 3.01 | 4.73 | 2.1 | 3.1 | 5.0 |
| GalCer−SM | 1.14 | 1.13 | | 2.0 | 0.9 | |
| GalCer−CHOL | 0.31 | 0.20 | | 0.3 | 0.3 | |
| CHOL−POPC | 0.58 | 0.82 | | 0.60 | 0.69 | |
| CHOL−SM | 0.14 | 0.10 | | 0.17 | 0.12 | |
| CHOL−GalCer | 0.09 | 0.08 | | 0.05 | 0.05 | |
| SM−POPC | 0.38 | 0.57 | | 0.37 | 0.50 | |
| SM−SM | 1.13 | 1.06 | | 1.12 | 1.13 | |
| SM−GalCer | 0.36 | 0.47 | | 0.3 | 0.2 | |
| SM−CHOL | 0.14 | 0.10 | | 0.17 | 0.12 | |
| POPC−SM | 0.37 | 0.28 | | 0.36 | 0.24 | |
| POPC−GalCer | 0.79 | 0.62 | 0.49 | 0.3 | 0.3 | 0.2 |
| POPC−CHOL | 0.58 | 0.41 | | 0.60 | 0.33 | |

[a] Errors are estimated at less than 5%.

**Table 8. Average Number of Charge Pairs from One Molecule of a Species to Molecules of the Second Type[a]**

| | system | | | | | |
|---|---|---|---|---|---|---|
| molecule pair | $I_{10}$ | $II_{10}$ | $III_{10}$ | $I_5$ | $II_5$ | $III_5$ |
| GalCer−POPC | 2.39 | 3.99 | 4.8 | 2.71 | 3.55 | 5.31 |
| GalCer−SM | 1.89 | 1.68 | | 2.45 | 1.48 | |
| CHOL−POPC | 0.48 | 0.76 | | 0.65 | 0.38 | |
| CHOL−SM | 0.50 | 0.26 | | 0.59 | 0.42 | |
| SM−POPC | 2.09 | 3.21 | | 3.71 | 4.76 | |
| SM−SM | 3.91 | 3.32 | | 3.76 | 3.54 | |
| SM−GalCer | 0.60 | 0.69 | | 0.37 | 0.29 | |
| SM−CHOL | 0.52 | 0.26 | | 0.59 | 0.42 | |
| POPC−POPC | 2.98 | 3.51 | 4.6 | 2.93 | 3.68 | 4.35 |
| POPC−SM | 2.04 | 1.6 | | 3.62 | 2.46 | |
| POPC−GalCer | 0.74 | 0.83 | 0.50 | 0.40 | 0.36 | 0.26 |
| POPC−CHOL | 0.48 | 0.38 | | 0.65 | 0.20 | |

[a] Errors are estimated at less than 5%.

## DISCUSSION

**Membrane Dimensions and Order Parameters.** The average area per lipid of the liquid-ordered (systems I and II) and liquid-disordered lipid bilayers (systems III) does not change or decreases very slightly as the concentration of GalCer is increased. The change is most visible in the liquid-disordered system, with a shift of 0.02 $nm^2$ between the different systems. However, when comparing with previous simulations of similar bilayer systems without GalCer,[40] it can be seen that the changes are very small and, with the exception of $III_{10}$, fall within error boundaries. So, in essence, the changes in the area per lipid caused by GalCer are minimal.

The same clearly does not hold for bilayer thickness. There is an increase of a few angstroms in bilayer thickness for both of the liquid-ordered systems caused by the addition of GalCer. For II the change is exceptionally large as the bilayer thickness ranges from 4.29 nm for a similar simulation without GalCer,[40] through 4.42 nm for a system with 5%, up to 4.66 nm for a system with 10% GalCer. The change is almost as large for the systems I, where it

shifts from 4.40 nm for a system without GalCer[40] to 4.56 nm for 5% GalCer and 4.66 nm for 10% GalCer.

The electron density profiles show that GalCer lies deeper in the bilayer and the galactosyl headgroup resides under the phosphoryl headgroups of POPC and SM.[21] GalCer seems to cause the thickening of the bilayer by pushing the phospholipids outward through hydrogen bonding.[21] As the concentration of GalCer increases, they are able to push the phospholipids further outward, thus causing the bilayer to thicken.

The hydrocarbon chain order parameters show a slight increase in chain ordering caused by the increase of GalCer from 5 to 10%. The changes are small, as can be seen by comparing the average order parameter of the 10% systems for carbons 5−7 (counting toward the chain ends) with those obtained for similar systems without GalCer.[40] For the systems I the average order parameter is the same (0.41), while for II it changes from 0.36 to 0.37 with the addition of GalCer, and for III (comparison to similar POPC system, with trace amounts of SM and CHOL) from 0.18 to 0.19.

**Interdigitation.** As the amount of GalCer in the simulated lipid bilayers is increased from 5 to 10%, interdigitation of the hydrocarbon chains in both of the liquid-ordered systems (I, II) decreases slightly. This is quite surprising, since the interdigitation is mainly caused by the GalCer molecules, as can be concluded from electron density profiles across the bilayers (see Figure 3).[21] In a system where there is only a small amount of GalCer, the GalCer molecules are not able to push the other lipids outward without being pushed inward and thus causing their chain ends to interdigitate with those of the opposite monolayer. As the concentration of GalCer increases, the situation changes, as they are more capable pushing the phospholipids more strongly upward and are not forced to interdigitate as much with the other monolayer.

The effect of interdigitation with the addition of GalCer is most likely dependent on the length of the hydrocarbon chains. Naturally occurring sphingolipids have either saturated or unsaturated chains which range in length from 16 to 24 carbons. As both SM and GalCer studied here have saturated 16 carbon acyl chains, they are from the shorter end of the spectrum. Interdigitation in sphingolipids is proportional to the length of the acyl chain,[43,48,49] and thus the molecules studied here are not as likely to extensively interdigitate as longer chains would be.

The measure used here for interdigitation in a bilayer has previously been used to study bilayer systems consisting of ceramide, cholesterol, and free fatty acids.[44] The numerical values obtained here (0.22−0.53 nm) are smaller than the ones obtained for those systems (1−3 nm). The differences in the amount of interdigitation are evident when comparing bilayer profiles and are caused by the significant differences both in hydrocarbon chain length (16 vs 24) and simulation temperature (310 vs 340 K).

**Hydrogen Bonding and Charge Pairs.** Hydrogen bonding in the studied systems is clearly dominated by GalCer, which unlike phospholipids is able to form a large number of hydrogen bonds through its sugar headgroup. As the concentration of GalCer is increased from 5 to 10% the total number of hydrogen bonds is increased considerably. The increase is approximately 20% in the systems I, almost 60% in II, and around 100% in III. There are no major changes in the number of hydrogen bonds per molecule, but rather the change is almost solely caused by the increase in the number of GalCer molecules.

After GalCer, the second largest contributor to hydrogen bonding is SM. However, over half of the hydrogen bonds formed by SM are to other SM molecules, while GalCer−GalCer bonds are much less frequent, less than 1 in 10. Therefore, it could be possible that quite a large part of the hydrogen bonds from SM may actually be intramolecular. This is supported by the fact that the number of SM−SM bonds closely matches that found for intramolecular SM−SM bonds in a previous study.[50]

The results obtained here show that CHOL prefers hydrogen bonding with both POPC and GalCer over SM. The number of hydrogen bonds for a given CHOL−POPC pair is three times, and CHOL−GalCer two times, as large as that for CHOL−SM. This finding supports previous results[50] in showing that CHOL tends to favor hydrogen bonding with POPC over SM in mixed lipid bilayers.

Unlike the number of hydrogen bonds, the total number of charge pairs formed in the systems slightly decreases with the addition of GalCer from 5 to 10%. The decrease is 17% for I, 8% for II, and 6% for III. This change is mainly caused by the decrease in charge-pair-forming phosphorylcholine headgroups. The change in the number of charge pairs is less significant than the change in hydrogen bonds, and has less effect, since the binding energy of a charge pair between these types of molecules is expected to be approximately one-third of that for a proper hydrogen bond.[50] Therefore, the total binding energy from both hydrogen bonds and charge pairs increases as more GalCer is added.

In the liquid-ordered systems, CHOL molecules tend to be bonded, on average, to other lipids through both one hydrogen bond and one charge pair. The results obtained here show CHOL favoring charge pairs with POPC and SM equally. This differs from results obtained previously,[50] which indicated that CHOL would prefer charge pair formation with SM over POPC. Additionally, the relative number of both CHOL−POPC hydrogen bonds and charge pairs seems to correlate somewhat with how ordered the system is, as the least ordered 4-component system ($II_S$ with 5%) has the smallest number of both.

**Lateral Diffusion.** Clearly the largest effect caused by the addition of GalCer to lipid bilayers is a considerable decrease in lateral diffusion for all lipid components. This is clearly seen by looking at the larger picture formed by the 5 and 10% systems, together with previous results for similar systems without GalCer.[40]

For the systems II the connection between the amount of GalCer and the lateral diffusion coefficient is the clearest. When 5 mol % of GalCer is added, the average lateral diffusion coefficient of lipids drops by approximately 20%,[21] and with 10 mol % of GalCer the diffusion coefficient drops by almost 80% in comparison to a system without GalCer.[40] Effectively, the addition of only 10% GalCer causes a shift of nearly 1 order of magnitude in the diffusion of the system. In both of the systems with GalCer there is a notable difference in the diffusion coefficients for different lipid components that is absent without GalCer. GalCer is the slowest lipid component in both of these systems, CHOL the fastest, and the value of SM resides between these two. In the 5% system POPC diffuses at the same rate as CHOL, but with the addition of more GalCer to 10% it shifts to diffusing at almost the same speed as SM.

In the case of I, the matter is a bit more complicated, since with the addition of 5% GalCer the average diffusion coefficient remains constant (within error bars) or even increases compared to a membrane without GalCer.[21,40] As the number of GalCer molecules is increased to 10 mol %, the behavior of the system changes completely, with the average diffusion coefficient decreasing by 75% when compared with the system without GalCer. Again, we have a

decrease of nearly 1 order of magnitude. In the 10% system all of the lipids now diffuse at the same slow speed, which is the same as for GalCer in the system $II_{10}$. The addition of more GalCer to the system allows it to bond more with the other lipids, leading to a more uniform diffusion of all the lipids in the bilayer.

When comparing the liquid-disordered systems III with 5 and 10% GalCer to a similar system without GalCer, but with trace amounts of SM and CHOL,[40] we find very similar behavior to that in the liquid-ordered systems. As 5% of GalCer is added, the diffusion coefficient drops by approximately 20%.[21] When the number of GalCer molecules is increased to 10% the diffusion coefficient drops further, ending up at approximately 50% of the value found without GalCer. The change in diffusion coefficient caused by GalCer appears to be slightly smaller for the liquid-disordered system. In both the 5% and 10% systems GalCer has a smaller diffusion coefficient than POPC.

According to these results, even quite a small amount of GalCer can drastically reduce the diffusion speed in a bilayer. The decrease in diffusion cannot be attributed to interdigitation. While interdigitation may play some role in slowing down the diffusion of the system, the observed huge drop in diffusion between the 5% and 10% systems is still caused by something else.

We conclude that GalCer affects the diffusion of the lipids by forming webs of hydrogen bonds that bind the lipids in place. This view is supported by the hydrogen bond data in Table 7, which shows that the strongest intermolecular bonding in terms of hydrogen bonds takes place between GalCer and POPC, and GalCer and SM, while the third but weaker interaction appears between POPC and cholesterol. This suggests that GalCer acts as a hub which is coupled to several POPC and SM molecules, forming local slowly moving clusters that are occasionally bridged to cholesterol via POPC. The results in Table 4 are consistent with this view, showing that GalCer diffuses the slowest, followed by POPC and SM, while the lateral motion of cholesterol is the fastest of the four molecule types.

Further support for the importance of hydrogen bond patterns through GalCer is given by the fact that there is a marked increase in the total number of hydrogen bonds between the 5% and 10% systems, caused by the addition of GalCer. While there is also a drop in the total number of charge pairs between the 5% and 10% systems, this is not likely to have as large a role as the hydrogen bonds, since the charge pairs have a weaker binding energy,[50] and the total binding energy from both charge pairs and hydrogen bonds is expected to increase.

Finally, let us come back to the captivating finding that the lateral diffusion of cholesterol is the fastest among the four different lipid types. This is not entirely expected since both similar and opposite findings have been made in simpler fluid model membranes, such as two-component bilayers composed of CHOL and saturated PCs,[51−53] and three-component membranes of glycerophospholipids with minor amounts of sphingomyelin and CHOL.[40] In ternary raft-forming bilayers with considerable amount of cholesterol, the diffusion coefficients have been found to be essentially identical for all lipid types.[40,54] The smaller molecular weight of cholesterol suggests that its diffusion could be faster compared to phospho- and glycolipids. On the other hand, in saturated membranes, cholesterol is known to promote the ordering of lipids around it, and the ordered lipids could be expected to diffuse more slowly than the less ordered ones farther away from cholesterols. In the four-component membranes that we have studied in the present work, these principles likely contribute but the role of GalCer in creating locally bonded clusters is presumably more prominent. As CHOL is rather weakly hydrogen bonded or charge paired to GalCer, POPC, and SM, its diffusion becomes relatively faster compared to the other molecules that we consider to form transient local clusters moving partly together.

**Interleaflet Friction.** The diffusion of the two monolayers in relation to each other is thought to be closely linked to interleaflet friction (viscosity) of the bilayer,[43] which in turn should be closely associated with interdigitation. The studied systems (especially the system $I_{10}$) exhibit such high ordering that the monolayers are not able to freely slide against each other, but rather may be weakly bound to one another. Generally, viscosity is thought to be dependent on the interdigitation of the lipids in the bilayers, with higher values of interdigitation causing stronger friction,[43] but in the systems studied here the connection between the two is not clear.

The values obtained for the systems I and III seem to be more in line with the diffusion of individual lipid components than with interdigitation between the two monolayers, as the viscosity decreases with 10% GalCer, while the interdigitation decreases. This result is quite dependent on the time period for which the diffusion between the two layers is calculated. As the statistics for the results is quite poor, we think that no strong conclusions on the behavior of the systems interleaflet friction can be derived from these results. What we can conclude qualitatively is that interleaflet friction becomes stronger for increasing GalCer concentration, but quantitatively the issue remains to be clarified.

**Autocorrelation Functions.** The results for the rotational autocorrelation functions generally indicate that there is no major change in the dynamics of the rotational motion caused by the increase in GalCer from 5 to 10%. While the headgroups, interfacial areas, and hydrocarbon chains are slightly more restricted in their movement, the actual speed at which they are able to respond to changes in their surroundings is not considerably altered. It was found in a previous study that the addition of cholesterol to lipid bilayers dramatically slows down rotational movement of the other lipids, which is seen as slower relaxation of the autocorrelation functions.[47] According to the results obtained here, the addition of GalCer does not have a similar effect on the other lipids, but rather mainly affects their lateral diffusion. The results for the systems in this work exhibit much longer relaxation times for all of the different rotational movements,[47] due to the systems being more ordered and at a lower temperature.

## SUMMARY

Our results show that the addition of galactosylceramide to a membrane containing phospholipids and cholesterol has a strong effect on the dynamics of the system, mainly by slowing down lateral diffusion. This supports the experimental findings of Maunula et al.[12] which indicated that ordered membrane domains containing cholesterol and sphingomyelin were thermally more stable when glycosphingolipids were introduced to the system. In addition to slowing down the movement of individual molecules as more GalCer is added to the system, interleaflet friction also grows, while the amount of interdigitation decreases at the same time. The effects on chain order and packing of the molecules, as seen in the area per lipid and $S_{CD}$, are on the other hand quite minimal; only the less ordered systems show noticeable increase. Bilayer thickening correlates clearly with the decreasing interdigitation. Based on our results, the most plausible explanation for the effect of GalCer on the dynamics of a phospholipid−cholesterol membrane is the

larger number of intermolecular hydrogen bonds, which bind the molecules more strongly in their place.

## AUTHOR INFORMATION

**Corresponding Author**
*E-mail: Ilpo.Vattulainen@tut.fi.

## ACKNOWLEDGMENT

We thank the financial support by the Glycoscience Graduate School GGS (A.H.) and the Academy of Finland (A.H., T.R., I.V.). We also thank the HorseShoe (DCSC) supercluster at the University of Southern Denmark and the Finnish IT Centre for Scientific Computing (CSC) for computer resources.

## REFERENCES

(1) Hakomori, S. *Biochim. Biophys. Acta* **2008**, *1780*, 325–346.
(2) Degroote, S.; Wolthoorn, J.; van Meer, G. *Sem. Cell Dev. Biol.* **2004**, *15*, 357–387.
(3) Róg, T.; Vattulainen, I.; Bunker, A.; Karttunen, M. *J. Phys. Chem. B* **2007**, *111*, 10146–10154.
(4) Hinz, H.-J.; Kuttenreich, H.; Meyer, R.; Renner, M.; Fründ, R. *Biochemistry* **1991**, *30*, 5125–5138.
(5) Pike, L. J. *Biochem. J.* **2004**, *387*, 281–292.
(6) Kasahara, K.; Sanai, Y. *Biophys. Chem.* **1999**, *82*, 121–127.
(7) Hooper, N. M. *Mol. Membr. Biol.* **1999**, *16*, 145–146.
(8) Simons, K.; Ikonen, E. *Nature* **1997**, *387*, 569–572.
(9) Lingwood, D.; Simons, K. *Science* **2010**, *327*, 46–50.
(10) Rajendran, L.; Simons, K. *J. Cell Science* **2005**, *118*, 1099–1102.
(11) Schnaar, R. L.; Suzuki, A.; Stanley, A. In *Essentials of Glycobiology: Glycosphingolipids*, 2nd ed.; Varki, A., et al. , Eds.; Cold Spring Harbor Laboratory Press: New York, 2009; pp 129−141.
(12) Maunula, S.; Björkvist, Y. J. E.; Slotte, J. P.; Ramstedt, B. *Biochim. Biophys. Acta* **2007**, *1768*, 336–345.
(13) Björkvist, Y. J. E.; Nyholm, T. K. M.; Slotte, J. P.; Ramstedt, B. *Biophys. J.* **2005**, *88*, 4054–4063.
(14) Lingwood, D.; Binnington, B.; Rog, T.; Vattulainen, I.; Grzybek, M.; Coskun, U.; Lingwood, C. A.; Simons, K. *Nat. Chem. Biol.* **2011**, *7*, 260–262.
(15) Prinetti, A.; Loberto, N.; Chigorno, V.; Sonnino, S. *Biochim. Biophys. Acta* **2009**, *1788*, 184–193.
(16) Westerlund, B.; Slotte, J. P. *Biochim. Biophys. Acta* **2009**, *1788*, 194–201.
(17) Bjelkmar, P; Niemela, P. S.; Vattulainen, I; Lindahl, E. *PLoS Comput. Biol.* **2009**, *5*, e1000289.
(18) Shaw, D. E.; Maragakis, P.; Lindorff-Larsen, K.; Piana, S.; Dror, R. O.; Eastwood, M. P.; Bank, J. A.; Jumper, J. M.; Salmon, J. K.; Shan, Y. B.; Wriggers, W. *Science* **2010**, *330*, 341–346.
(19) Falck, E.; Rog, T.; Karttunen, M.; Vattulainen, I. *J. Am. Chem. Soc.* **2008**, *130*, 44–45.
(20) Niemela, P.; Miettinen, M. S.; Monticelli, L.; Hammaren, H.; Bjelkmar, P.; Murtola, T.; Lindahl, E.; Vattulainen, I. *J. Am. Chem. Soc.* **2010**, *132*, 7574–7575.
(21) Hall, A.; Róg, T.; Karttunen, M.; Vattulainen, I. *J. Phys. Chem. B* **2010**, *114*, 7797–7807.
(22) Tieleman, D. P.; Berendsen, H. J. C. *Biophys. J.* **1998**, *74*, 2786–2801.
(23) Niemelä, P.; Hyvönen, M. T.; Vattulainen, I. *Biophys. J.* **2004**, *87*, 2976–2989.
(24) Höltje, M.; Förster, T.; Brandt, B.; Engels, T.; von Rybinski, W.; Höltje, H. D. *Biochim. Biophys. Acta* **2001**, *1511*, 156–167.
(25) Bachar, M.; Brunelle, P.; Tieleman, D. P.; Rauk, A. *J. Phys. Chem. B* **2004**, *108*, 7170–7179.
(26) Martinez-Seara, H.; Róg, T.; Karttunen, M.; Reigada, R.; Vattulainen, I. *J. Chem. Phys.* **2008**, *129*, 105103.
(27) Martinez-Seara, H.; Róg, T.; Pasenkiewicz-Gierula, M.; Vattulainen, I.; Karttunen, M.; Reigada, R. *Biophys. J.* **2008**, *95*, 3295–3305.
(28) Berendsen, H. J. C.; Postma, J. P. M.; van Gunsteren, W. F.; Hermans, J. Interaction models for water in relation to protein hydration. In *Intermolecular Forces*; Pullman, B., Ed.; Reidel: Dordrecht, The Netherlands, 1981.
(29) Martinez, J. M.; Martinez, L. *J. Comput. Chem.* **2003**, *24*, 819–825.
(30) Berendsen, H. J. C.; van der Spoel, D.; van Drunen, R. *Comput. Phys. Commun.* **1995**, *91*, 43–56.
(31) Lindahl, E.; Hess, B.; van der Spoel, D. *J. Mol. Model.* **2001**, *7*, 306–317.
(32) van der Spoel, D.; Lindahl, E.; Hess, B.; Groenhof, G.; Mark, A. E.; Berendsen, H. J. C. *J. Comput. Chem.* **2005**, *26*, 1701–1719.
(33) Berendsen, H. J. C.; Postma, J. P. M.; van Gunsteren, W. F.; DiNola, A.; Haak, J. R. *J. Chem. Phys.* **1984**, *81*, 3684–3690.
(34) Nose, S. *Mol. Phys.* **1984**, *52*, 255–268.
(35) Hoover, W. *Phys. Rev. A* **1985**, *31*, 1695–1697.
(36) Nose, S.; Klein, M. L. *Mol. Phys.* **1983**, *50*, 1055–1076.
(37) Parrinello, M.; Rahman, A. *J. Appl. Phys.* **1981**, *52*, 7182–7190.
(38) Hess, B.; Bekker, H.; Berendsen, H. J. C. *J. Comput. Chem.* **1997**, *18*, 1463–1472.
(39) Karttunen, M.; Roettler, J.; Vattulainen, I.; Sagui, C. In *Current topics in membranes: Computational modeling of membrane bilayers*; Feller, S. E., Ed.; Elsevier: Amsterdam, 2008; pp 44−89.
(40) Niemela, P.; Ollila, S.; Hyvonen, M. T.; Karttunen, M.; Vattulainen, I. *PLoS Comput. Biol.* **2007**, *3*, 304–312.
(41) Patra, M.; Karttunen, M.; Hyvonen, M. T.; Falck, E.; Lindqvist, P.; Vattulainen, I. *Biophys. J.* **2003**, *84*, 3636–3645.
(42) Patra, M.; Karttunen, M.; Hyvonen, M. T.; Falck, E.; Vattulainen, I. *J. Phys. Chem. B* **2004**, *108*, 4485–4494.
(43) Niemelä, P. S.; Hyvönen, M. T.; Vattulainen, I. *Biophys. J.* **2006**, *90*, 851–863.
(44) Das, C.; Noro, M. G.; Olmsted, P. D. *Biophys. J.* **2009**, *97*, 1941–1951.
(45) Pasenkiewicz-Gierula, M.; Róg, T.; Kitamura, K.; Kusumi, A. *Biophys. J.* **2000**, *78*, 1376–1389.
(46) Zhao, W.; Róg, T.; Gurtovenko, A. A.; Vattulainen, I.; Karttunen, M. *Biochimie* **2008**, *90*, 930–938.
(47) Martinez-Seara, H.; Róg, T.; Karttunen, M.; Vattulainen, I.; Reigada, R. *J. Phys. Chem. B* **2009**, *113*, 8347–8356.
(48) Mehlhorn, I. E.; Florio, E.; Barber, K. R. *Biochim. Biophys. Acta* **1988**, *939*, 151–159.
(49) Barenholz, Y.; Thompson, T. E. *Chem. Phys. Lipids* **1999**, *102*, 29–34.
(50) Aittoniemi, J.; Niemela, S.; Hyvönen, M. T.; Karttunen, M.; Vattulainen, I. *Biophys. J.* **2007**, *92*, 1125–1137.
(51) Falck, E.; Patra, M.; Karttunen, M.; Hyvonen, M. T.; Vattulainen, I. *Biophys. J.* **2004**, *87*, 1076–1091.
(52) Hofsas, C.; Lindahl, E.; Edholm, O. *Biophys. J.* **2003**, *84*, 2192–2206.
(53) Scheidt, H. A.; Huster, D.; Gawrisch, K. *Biophys. J.* **2005**, *89*, 2504–2512.
(54) Oradd, G.; Westerman, P. W.; Lindblom, G. *Biophys. J.* **2005**, *89*, 315–320.